Septin-based readout of PI(4,5)P2 incorporation into membranes of giant unilamellar vesicles

Alexandre Beber, Maryam Alqabandi, Coline Prévost, Fanny Viars, Daniel Lévy, Patricia Bassereau, Aurélie Bertin, Stéphanie Mangenot

Septin-based readout of PI(4,5)P2 incorporation into membranes of giant unilamellar vesicles.

Alexandre Beber[1,2], Maryam Alqabandi[1,2], Coline Prevost[1,2], Fanny Viars[3], Daniel Levy[1,2], Patricia Bassereau[1,2] and Aurélie Bertin*[1,2], Stéphanie Mangenot*[1,2]

1- Laboratoire Physico Chimie Curie, Institut Curie, PSL Research University, CNRS UMR168, 75005, Paris, France
2- Sorbonne Université, 75005, Paris, France
3- Institut des maladies métaboliques et cardiovasculaires, UMR1048, Inserm/Université Paul Sabatier, 31432 Toulouse, France

* Both authors have equally contributed to the work

Corresponding author: Stephanie.mangenot@curie.fr and aurelie.bertin@curie.fr

Abstract:

Septins constitute a novel class of cytoskeletal proteins. Budding yeast septins self-assemble into non-polar filaments bound to the inner plasma membrane through specific interactions with L- α-phosphatidylinositol-4,5-bisphosphate (PI(4,5)P2). Biomimetic in vitro assays using Giant Unilamellar Vesicles (GUVs) are relevant tools to dissect and reveal insights in proteins-lipids interactions, membrane mechanics and curvature sensitivity. GUVs doped with PI(4,5)P2 are challenging to prepare. This report is dedicated to optimize the incorporation of PI(4,5)P2 lipids into GUVs by probing the proteins-PI(4,5)P2 GUVs interactions. We show that the interaction between budding yeast septins and PI(4,5)P2 is more specific than using usual reporters (phospholipase Cδ1). Septins have thus been chosen as reporters to probe the proper incorporation of PI(4,5)P2 into giant vesicles. We have shown that electro-formation on platinum wires is the most appropriate method to achieve an optimal septin-lipid interaction resulting from an optimal PI(4,5)P2 incorporation for which, we have optimized the growth conditions. Finally, we have shown that PI(4,5)P2 GUVs have to be used within a few hours after their preparation. Indeed, over time, PI(4,5)P2 is expelled from the GUV membrane and the PI(4,5)P2 concentration in the bilayer decreases .

1- INTRODUCTION

Septins are filamentous proteins that interact with actin and microtubules. Septins are now considered to be the fourth cytoskeletal member (Mostowy and Cossart 2012) and are thus concentrating increasing interest. Septins self-assemble into oligomeric cytoskeletal filaments that interact with the cytosolic leaflet of plasma membranes through specific interactions with the phosphoinositides lipids (Bertin et al. 2010; Bridges and Gladfelter 2014). As already shown by previous studies, the interaction between L- α-phosphatidylinositol-4,5-bisphosphate (PI(4,5)P2) lipids and *Saccharomyces cerevisiae* septins is specific and sensitive to the presence of PI(4,5)P2 in the membrane (Catimel et al. 2008; Rodríguez-Escudero et al. 2005). Septins are implicated into essential processes from cytokinesis to ciliogenesis, neuro-morphogenesis, spermiogenesis (Saarikangas and Barral 2011) and are thus involved and ill-regulated in cancers and neurodegenerative diseases (Hall and Russell 2004). Nevertheless, so far, only a handful of in vitro studies have attempted to dissect the function of septins (Bertin et al. 2010) (Bridges and Gladfelter 2014; Bridges et al. 2016). Hence, there is a current need in the septin field for specific biomimetic in vitro tools.

Giant Unilamellar Vesicles (GUVs) have been first described several decades ago (Reeves and Dowben 1969) and have been thoroughly employed since then in biophysical assays (Evans et al. 1980; Walde et al. 2010). GUVs are widely used to study protein lipid interactions (Kahya 2010), membrane mechanics (Evans et al. 1980) and curvature sensitivity (Lagny and Bassereau 2015). Depending on their lipid composition, biomimetic membranes are challenging to produce. For instance, the incorporation of charged lipids within GUV is not straightforward. It is thus difficult to precisely control the amount of negatively charged lipids in the membrane since they insert with a low efficiency within supported bilayers (Kunze et al. 2009; Cha et al. 2006) or GUVs (Bucher et al. 1998; Rodriguez et al. 2005). Working with phosphoinositides is particularly challenging and several reports were focused on the issue of phosphoinositide incorporation into vesicle membranes (Carvalho et al. 2008; Moens and Bagatolli 2007).

Phosphoinositides are essential *in vivo* and are able to recruit a number of proteins at the membrane. Even though phosphoinositides represent a small fraction of the total cellular phospholipids, they are essential for cell viability. Among phosphoinositides, PI(4,5)P2 is the most abundant phosphoinositide of the inner leaflet in the plasma membrane. PI(4,5)P2 alters the physical properties of membranes such as curvature and elasticity (Rusinova et al. 2013) and is involved in a large variety of events such as membrane trafficking (Martin 2001), cell

motility (Golub and Caroni 2005) or cell signaling (Heo et al. 2006). The use of in vitro model membranes increases tremendously our understanding of lipid and protein interactions. However, it is of crucial importance to control and check the quality of the synthetic model membrane systems (Czogalla et al. 2014). This report has been motivated by our recurrent observation of the irreproducibility of the binding efficiency of proteins to biomimetic PI(4,5)P2 membranes.

Synthetic PI(4,5)P2 labeled with fluorophores is often used to check the incorporation of PI(4,5)P2 in a membrane. However, the fluorescent dye placed either on the head or on the tail, may modify substantially the lipid behavior (Carvalho et al. 2008). Several PI(4,5)P2 protein reporters have been described such as antibodies (Thomas et al. 1999), specific peptides such as MARCKS (Aderem 1992; Hartwig et al. 1992) and PH domains proteins (Harlan et al. 1994) like the phospholipase Cδ1, (PLC-δ) (Lemmon et al. 1995). Antibodies induce clustering artifacts at least in vitro (Carvalho et al. 2008) and MARCKS or phospholipase C are also sensitive to other lipids like phosphatidylserine or phosphatidylcholine (Morton et al. 2013) (Pu et al. 2009). We found that budding yeast septins are more specific to PI(4,5)P2 than PLC-δ. We thus used septins as a probe to report for proper protein-PI(4,5)P2 interaction.

We have optimized the preparation of PI(4,5)P2 GUVs to achieve the highest septins-lipids interactions. To this end, within the scope of this work, we propose a systematic study, which compares different methods for the preparation of such GUVs. We also tested the GUVs aging and the incubation time of proteins. We have focused our report on three main methods: gel-assisted swelling, electro-formation on planar indium tin oxide (ITO)-coated slides and electro-formation on platinum wires.

We found that the most reliable GUV-preparations are obtained after electro-formation on platinum wires in the presence of salt. Besides, PI(4,5)P2 GUVs need to be used within two hours after their production. We expect that this work will be of great use for the septin community as well as for all researchers investigating the interaction of proteins with membranes containing PI(4,5)P2.

2- MATERIAL AND METHODS

2.1 Septin complex expression and purification

Yeast-septins complexes containing Cdc11, His_6-Cdc12, GFP-Cdc10 and Cdc3 were co-expressed in Escherichia coli and purified as described in details elsewhere (Bertin and Nogales

2016). Briefly, septins are purified by immobilized nickel affinity, size exclusion and ion exchange chromatography. A Cdc11_His_6-Cdc12_Cdc3_GFP-Cdc10_GFP-Cdc10_Cdc3-His_6-Cdc12_Cdc11 fluorescent and palindromic complex is thus obtained.

2.2 PLC-δ expression, purification and labelling

PLC-δ has been prepared as described in (Picas et al. 2014) and was a gift from B. Goud. Proteins were provided at 2 $mg.mL^{-1}$ in 0.1 M sodium bicarbonate buffer containing 100 mM NaCl. PLC-δ were incubated with 5 M (Molarity) excess of Alexa 488-succinimidyl-ester (Thermo-Fisher) to fluorescently label the proteins. The excess of free dye was removed by chromatography on a desalting column PD-10. The final protein concentration was equal to 1.5 $mg.mL^{-1}$.

2.3 Material

L-α-phosphatidylcholine (EPC), 1,2-dioleoyl-*sn*-glycero-3 phosphoethanolamine (DOPE), 1,2-dioleoyl-*sn*-glycero-3-phospho-L-serine (DOPS), brain L-α-phosphatidylinositol-4,5 bisphosphate (PI(4,5)P2), PI(4,5)P2: GloPIPs BODIPY TMR-PtdIns(4,5)P2, C16 (red PI(4,5)P2), 1-oleoyl-2-{6-[4-(dipyrromethene boron difluoride) butanoyl] amino} hexanoyl-*sn*-glycero-3-phosphoinositol-4,5-bisphosphate (TopFluor PI(4,5)P2), cholesterol, and synthetic lipid standards. 1-heptadecanoyl-2-(5Z,8Z,11Z,14Z-eicosatetraenoyl)-sn-glycero-3-phospho-(1'-myo-inositol-3',5'-bisphosphate) (PIP2 17:0-20:4) and 1-heptadecanoyl-2-(5Z,8Z,11Z,14Z-eicosatetraenoyl)-sn-glycero-3-phospho-(1'-myo-inositol-4'-phosphate) (PIP 17:0-20:4) were purchased from Avanti Polar Lipids (Albaster, AL, USA). BODIPY® TR Ceramide and Oregon-green 1,2-Dihexadecanoyl-*sn*-Glycero-3-Phosphoethanolamine (Oregon Green® 488 DHPE) was purchased from Thermo Fischer Scientific (Courtaboeuf, France). All lipids stocks are kept in argon and discard after 3 months to minimize oxidation.

Liquid chromatography solvent Acetonitrile HPLC-grade (ACN), Trimethylsilyl diazomethane 2M in hexane (TMSD), Methanol HPLC-grade (MeOH), Formic Acid (FA), Chloroform and Polyvinyl alcohol (PVA) were purchased from Sigma Aldrich. Acetic acid (AA) was from Fluka.

2.4 Mass spectrometry

Solutions of lipids resuspended at 1 $mg.mL^{-1}$ in an aqueous buffer (10 mM Tris-HCl, pH 8) were kept at 4°C and flash frozen at increasing time points from their initial resuspension. The samples were subsequently analyzed by mass spectrometry (Maldi-TOF).

2.5 Lipid extraction

Briefly an acidic extraction was performed on sample according to Clark's method (Clark et al. 2011) in presence of internal standards PIP 17:0-20:4 (20 ng) and PIP2 17:0-20:4 (20 ng). A solution of TMSD (2 $Mol.L^{-1}$) in hexane (50 µL) was added to the homogenate to obtain yellow-colored solutions at room temperature for 10 min. Extreme care should be taken when handling it. For this reason, methylation by TMSD has been carried out in a fume hood, with the use of adequate personal safety equipment. Addition of acetic acid (6 µL) quenched the methylation and afforded colorless samples. The lower phase was collected, washed twice and dried under azote, then dissolved in 30 µL MeOH/H2O (2:1). The extract was then stored at −20 °C before LC-MS/MS analysis.

2.6 Liquid chromatography mass spectrometry

High performance liquid chromatography was performed using an Agilent 1290 Infinity (Agilent Technologies) equipped with an auto sampler, a binary pump and a column oven.

The analytical column was an Acquity UPLC BEH300-C4 (100 x 1.0 mm, 1,7 µm) (Waters) maintained at 22 °C. The mobile phases consisted of Water, FA (99.9:0.1;v/v) (A) and ACN, FA (99.9:0.1, v/v) (B). The gradient was as follows: 45% B at 0 min, 100% B at 5 min, 100% B at 8 min, 45% B at 9 min, 45% B at 10 min. The flow rate was 0.1 $mL.min^{-1}$. The auto sampler was set at 5 °C and the injection volume was 10 µL. The HPLC system was coupled on-line to an Agilent 6460 triple quadrupole MS (Agilent Technologies) equipped with electrospray ionization source. Electrospray ionization (ESI) was performed in positive ion mode. After optimization, the source parameters used were as follows: source temperature was set at 250°C, nebulizer gas (nitrogen) flow rate was 8 $L.min^{-1}$, sheath gas temperature was 150°C, sheath gas (nitrogen) flow rate was 3 $L.min^{-1}$ and the spray voltage was adjusted to + 4000 V. The collision energy optimums for derived PIP (36:2) and derived PIP2 (36:2) were 30 eV.

Analyses were performed in Selected Reaction Monitoring detection mode (SRM) using nitrogen as collision gas. Finally, peak detection, integration and quantitative analysis were done using MassHunter QqQ Quantitative analysis software (Agilent Technologies).

2.7 GUVs preparation

GUVs were formed using three different methods: (i) Electroformation on planar ITO slides (Angelova et al. 1992) (ii) gel-assisted swelling on polyvinyl alcohol (PVA) (Weinberger et al. 2013), method referred to as PVA method in the text and (iii) electro-formation on platinum wires (Aimon et al. 2011; Garten et al. 2015). Vesicles were formed from a mix containing EPC, 10% DOPS, 10% DOPE, 15% cholesterol, 0.5% Bodipy-TR-ceramide, and various amounts of PI(4,5)P2 lipids up to 10%. In some experiment, the Bodipy-TR-ceramide was replaced by fluorescent PI(4,5)P2: GloPIPs BODIPY TMR-PtdIns(4,5)P2, C16 (for the red PI(4,5)P2) and TopFluor PI(4,5)P2 (for the Green PI(4,5)P2) at 0.5% (w:w) in the final GUV composition. All percentages of lipid composition are expressed in molar fraction.

For electro-formation on planar ITO slides, 10 µL of the lipid mixture prepared at 1 $mg.mL^{-1}$ in chloroform were deposited on the conducting side of two ITO slides. The organic solvent was then evaporated for 30 min under vacuum. The two slides were then sealed (conducting sides facing each other) to obtain a hermetic chamber filled with growth buffer A (10 mM Tris pH 7.6, 150 mM sucrose). The chamber was then plugged to an AC voltage equal to 1 V at 10 Hz for 1 hour. After formation, GUVs were collected by gentle pipetting of 20 µL of solution in the chamber.

For electro-formation on platinum wires, 4-5 µL of the lipid mixture at 3 $mg.mL^{-1}$ were spotted on two platinum wires mounted in a custom-made teflon chamber (Garten et al. 2015). The droplets were dried under vacuum for 30 minutes. The chamber was filled with growth buffer B (10 mM Tris pH7.6, 50 mM NaCl, 50 mM sucrose) and subjected to an AC voltage equal to 350 mV at 500 Hz for 6 hours or 250 mV at 500 Hz for 12-16 hours. GUVs were collected by pipetting 20-30 µL of solution along each platinum wire.

For formation on PVA, a PVA solution at 5 % (w/w) in water was spread on a coverslip. After PVA polymerization, 10 µL of the lipid mixture at 1 $mg.mL^{-1}$ were deposited and dried for 30 min under vacuum. The lipids were rehydrated with 1 mL of growth buffer B for at least 1h. GUVs were then detached by gentle shaking of the chamber. 30 µL of the solution were then harvested to collect GUVs.

After the growth, GUVs were transferred in an iso-osmotic observation buffer (10 mM Tris pH 7.6, 75 mM NaCl).

2.8 Influence of the external buffer composition

To test the effect of monovalent salt in the external buffer on the septin binding, GUVs were grown by electro-formation on platinum wires with an internal buffer composed of 10 mM Tris pH 7.6, 50 mM NaCl and various amounts of sucrose to match the external buffer osmolarity. The external buffer was composed of 10 mM Tris pH 7.6 and various amount of NaCl ranging from 75 mM to 400 mM.

To test the effect of glucose in the external buffer, GUVs were grown by electro-formation on platinum wires with an internal buffer composed of 10 mM Tris pH 7.6, 50 mM NaCl, 200 mM sucrose. The external buffer composition was 10 mM Tris pH 7.6, 100 mM NaCl and 100 mM glucose or 10 mM Tris pH 7.6, 20 mM NaCl and 260 mM glucose.

2.9 Effect of the drying temperature

To test the effect of the temperature, during the drying step, on the electro-formation on platinum wires, the droplets of the lipid mixture were dried for 30 min under vacuum, either at room temperature or at 60°C. The lipid films were rehydrated and treated as described in the GUVs preparation section.

2.10 GUVs imaging

GFP-tagged septins previously diluted in the observation buffer were added in the observation chamber containing GUVs at 500 nM final concentration or at 1 µM (for the determination of the association constant). The chamber was previously incubated for 20 min with β-casein at 5 $mg.mL^{-1}$ diluted in the observation buffer to avoid adhesion of septin to the glass coverslip.

Confocal images were acquired on a Nikon Eclipse TE-2000 microscope equipped with a C1-confocal head with two laser lines (λ = 488 nm and λ = 543 nm) and a Nikon Plan Fluor 100× oil objective (1.3 NA) to image lipids and GFP-tagged septins signals. The confocal head is equipped with a bandpass filter (750-900 nm, RG9, Schott glass). A photomultiplier tube is used for detection.

2.11 Image analysis

Quantitative fluorescence analysis was performed as previously described to probe the unilamellarity of the GUVs (Aimon et al. 2011) and to extract the surface density of GFP-septins on the GUVs membrane. Images were analyzed using the Radial profile plug-in of ImageJ. The integrated fluorescence signal on the contour of the GUV is converted to protein

density as previously described (Sorre et al. 2012) using the Oregon-green DHPE lipid signals, incorporated in GUVs grown with electro-formation on ITO in buffer B, as a standard. The intensity of fluorescence was calibrated to allow for an absolute measurement of protein densities

3- RESULTS

3.1 Septins are good reporters to test PI(4,5)P2 incorporation

Several studies reported that septins bind preferentially to phosphoinotitides and notably to PI(4,5)P2 (Catimel et al. 2008; Zhang et al. 1999; Bertin et al. 2010). We thus wanted to check that septins could be indeed good reporters to test the incorporation of PI(4,5)P2 in the membrane.

To this end, GUVs containing EPC, 10 % DOPS, 10 % DOPE, 15 % cholesterol, 0.5 % Bodipy-TR-Ceramide and various amount of PI(4,5)P2 lipids were produced by electro-formation on platinium wires during 6 hours as previously used (Prévost et al. 2015). After their production, the GUVs were immediately collected and incubated with either a classical reporter for PI(4,5)P2: the PH domain of phospholipase C, PLC-δ labelled with Alexa 488, at 4.2 µM or with a GFP-septin bulk concentration of 100 nM in buffer. Increasing the PI(4,5)P2 concentration induced a proportional increase of green proteins, bound to the membrane (Figure 1.A). For PI(4,5)P2 concentrations above 6-8 %, the amount of proteins bound to the membrane was constant.

To quantify properly the interaction between the lipids and the proteins, it was crucial to ensure that GFP-septins in the bulk are in excess. To this end, we determined the dissociation constant (Kd) of septins bound to GUVs containing 8 % PI(4,5)P2. The GUVs were incubated with various concentrations of septins, ranging from 1 nM to 1 µM. For each septins concentration, the density of septins bound to the GUVs (N = 629) was determined from the fluorescence intensity of the GFP-tagged septin complex along the contour of the vesicles, as in (Sorre et al. 2012). The green fluorescence intensity was calibrated beforehand, allowing us to convert fluorescence intensities into surface density of septins. The image analysis methodology is detailed in the material and methods section. The resulting binding curve of septin density as function of the bulk septin concentration is presented on fig. 2. Increasing the septin concentration induced a higher fraction of septins bound to the membrane. For septin bulk concentrations above 300 nM, the fraction of septins on the membrane was almost constant. The dissociation constant determined from the sigmoidal curves inflection points was found to

be equal to 73 ± 9 nM. The Kd value was obtained by fitting the data with a Hill equation with n = 1.3 and a saturation density of 9200 μm^{-2} (Table 1). The low value of Kd for septins is the signature of a very strong interaction of septins with the lipid membrane. Previous experiments found that PLC-δ has a Kd value equal to 2 µM when interacting with PI(4,5)P2 lipids (Lemmon et al. 1995). All the experiments presented on fig. 1 were performed with a concentration of septins and PLC-δ above the Kd values. As a consequence, the saturation of the septin density in the GUV is not due to a too low protein concentration in the bulk solution. It is rather due to the fact the PI(4,5)P2 cannot be incorporated in membrane at concentration higher than 6-8%. The same effect has already been reported previously by Carvalho et al who found that only 8% PI(4,5)P2 could be incorporated in the GUV membrane (Carvalho et al. 2008).

Importantly, in the absence of PI(4,5)P2, there was no detectable interaction of septin with GUVs while PLC-δ interacted significantly with the membrane (fig 1.A (at 0% PIP2), and fig 1.B two first rows). PLC-δ displays small non-specific interaction in the absence of PI(4,5)P2. Septins are thus more sensitive to the PI(4,5)P2 than PLC-δ. The GUVs used in our assay contained 56.5% EPC and 10% DOPS. The phospholipase-C is known to interact strongly with PI(4,5)P2 as shown by figure 1.B (bottom row) but its conformation is tuned by interaction with PS headgroup (Uekama et al. 2007). Moreover, a small amount of PC lipids is known to activate the phosphoplipase C (Pu et al. 2009) and to trigger the mechanism for specific lipid interaction.

Thus, PLC-δ is a good reporter of PI(4,5)P2 incorporation in the GUV membrane, but septins appeared to be more selective and specific. Therefore, septins will be used as reporter in all the present work to optimize the incorporation of PI(4,5)P2 lipids.

The experiments described below are performed at a septin concentration of 200 nM to ensure membrane saturation by the proteins

3.2 Optimal interaction of septins with membranes is achieved when GUVs are electroformed on platinum wires

In vivo, multiple metabolic pathways, notably involving kinases, phosphatases and phospholipases, regulate the spatio-temporal concentration of PI(4,5)P2 in the membranes (Di Paolo and De Camilli 2006; Kwiatkowska 2010). The major route of production of PI(4,5)P2 is the phosphorylation by type I kinase of PI(4)P. It can also be produced but in fewer extent by phosphorylation of PI(5)P or by dephosphorylation of PI(3,4,5)P3. In a reverse process,

PI(4,5)P2 can be phosphorylated and dephosphorylated to produce PI(4)P, PI(5)P and PI(3,5,5)P3 (Kwiatkowska 2010). However, for *in vitro* assays, PI(4,5)P2 needs to remain stably inserted within the biomimetic GUVs bilayer and should not be hydrolyzed. We thus systematically assessed the influence of the GUVs growth method and parameters by probing the interaction between the membrane and the yeast septins, assuming this directly reflected the incorporation and stability of PI(4,5)P2 in the bilayer.

First, we compared different methods to produce GUVs focusing our work on electro-formation on planar ITO slide (Fig. 3.A), gel-assisted swelling on PVA (Fig. 3.C) and electro-formation on platinum wires (Fig. 3.B). The inverse emulsion method has been left out, as GUV containing charge lipids produced with this method can contain oil in their membrane (Prévost et al. 2015) .

Growth on ITO slides has been the most established method of GUVs production, but it precludes the use of physiological salt in the buffer. GUVs were grown on ITO slides in buffer A (see Material and Methods for details and (Angelova et al. 1992)) (Figure 3.A) and incubated with septins in buffer B immediately after growth. As shown in fig. 3.D (upper row), no binding of GFP-septin was detected on the ITO-grown GUVs for PI(4,5)P2 concentrations up to 10% ($N_{experiments} = 3$).

We then compared the quality of the GUVs production of two alternative methods, gel-assisted on PVA and electro-formation on platinum wires, methods which both allow the presence of salt in the growth buffer. The interaction between the GUVs containing 8% PI(4,5)P2 and the septins is shown in fig. 3.E (middle and bottom rows). For GUVs produced by the gel-assisted swelling on PVA (Fig. 3.E, bottom row), referred as PVA-GUVs, the density of septins was equal to 8200 ± 1400 septins/μm^2 (N=212), corresponding to a high membrane coverage of approximately 98% (if one consider that septin surface area is 30 nm*4nm (Bertin et al. 2008)). For GUVs produced by electro-formation on platinum wires (fig. 3.E, middle row), Ptw-GUVs, the density was slightly lower and was equal to 5200 ± 600 septins/μm^2 (N=205). Both the PVA and the platinum wire methods were performed in the presence of salts. Since PI(4,5)P2 is a negatively charged lipid, the absence of salt during the growth presumably prevented the PI(4,5)P2 from being properly incorporated within vesicles. To test for salt requirement, we thus produced GUVs with either gel-assisted (Fig. 3.D, bottom row) and platinum wire (Fig. 3.D, middle row) in Buffer A (without any salt) and incubated with septins in Buffer B. Here again, no interaction was detected between the membrane and the septins (Figure 3.D),

implying that salt is indeed required in the growth buffer to properly incorporate PI(4,5)P2 in the membrane.

The morphology of the vesicles was analyzed in more details. In our hands, we found that only 15 % of the PVA-grown vesicles were unilamellar without any defect (patch of lipids attached to the GUV, non-uniformity, lipids trapped inside the vesicle…). A gallery of vesicles showing typical defects is displayed in fig. 3.G. 35 % of the vesicles displayed some defects and the majority of them (50 %) were multilamellar. Conversely, in the case of electro-formation on platinum wires, 58 % of the vesicles were unilamellar, 20 % displayed some defects and 22 % were multilamellar (fig. 3.F) (N=212).

The average density of GFP-septins was higher on PVA-GUVs than Ptw-GUVs, possibly because of the high number of multilamellar PVA-vesicles. Indeed, considering only the unilamellar vesicles, the average septins density was equal to 5400 ± 1300 septin.μm^{-2}, similar to the septin density on Ptw-GUVs. To explain this difference, we propose that in multilamellar vesicles, the different internal bilayers might provide a protective reservoir of PI(4,5)P2 for the most external bilayer which, being in direct contact with a large amount of buffer, loses PI(4,5)P2 by solubilization or degradation. This exchange could occur by a flip flop exchange of PI(4,5)P2 from one layer to another.

Out of the three GUV preparation methods we have tested, in our hand, electro-formation on platinum wires appear to be the most satisfactory: the affinity of septins with those vesicles is high, and a majority of the vesicles is unilamellar without defects**.** We thus decided to pursue our investigations using GUVs grown with electro-formation (Ptw-GUV) and optimized all the parameters to achieve a high septin-membrane interaction.

3.3 Optimization of the growth conditions on platinum wire for optimal septin-membrane binding

To get more insights into the conditions ensuring optimal binding we have tested several parameters that can be tuned for GUVs production: (1) the presence of another negatively charged lipid (DOPS), (2) the drying temperatures (3) the duration of the electro-formation process, the environmental buffer (salt and glucose), and (4) the voltage applied throughout the electro-formation process.

First, we tested the role of another negatively charged lipid, DOPS, to probe the role of non-specific electrostatic interactions on septin binding. In the presence of 10 % PS but without any PI(4,5)P2, septins did not interact at all with vesicles. In the presence of 10 % DOPS and 8 %

PI(4,5)P2 the septin density was equal to 5200 ± 600 septins.μm^{-2}. This value dropped to 3300 ± 700 septins.μm^{-2} when no PS was inserted in the membrane (N=65). The septin-membrane interaction was therefore specific to PI(4,5)P2 but was facilitated when the density of negative charges is higher on the membrane.

Second, we tested the drying condition of lipids after deposition on the wires. In previous reports, drying of the organic solvent after deposition of the lipids on platinum wires and growth of the vesicles were carried out at 60°C to ensure a complete mixing of lipid components (Liu and Fletcher 2006; Gokhale et al. 2005). As shown in Table 2, the septin density on GUVs was higher when the evaporation of the solvent was performed in vacuum or in air at room temperature than when it was carried out at 60°C (respectively 5200 ± 600 and 6400 ± 1000 compared with 2400 ± 300 septins/μm^2) (N=83); The growth was then performed at 4°C.

Third, we have varied the electro-formation parameters (voltage and growth duration) that optimized both the binding of septins onto GUVs and the quality of the vesicles. The growth duration was varied from 6 to 16 hours at a constant peak-to-peak voltage of 350 mV. For growth time below 6 hours, barely any GUVs were obtained. Above 6 hours, the production yield was satisfactory and we observed that the septin density on GUVs remained constant independently of the growth duration (fig. 4.A). However, the diameter of the vesicles decreased slightly with growth time (fig. 4.B) and the quality of the GUVs also deteriorated: both the fraction of multilamellar and defective vesicles increased with time (fig. 4.C). As a conclusion, the optimal growth time was 6 hours.

We also systematically varied the applied voltage. At a voltage above 450 mV, no growth occurred, probably because the heat generated by the electrical current on the wires induced severe degradation of the lipids. For lower voltages and for a growth time of 16 hours, the binding of septin onto GUVs was enhanced with increasing voltage (fig. 5.A). Previous report showed that with shorter growth time and higher voltage it was possible to achieve the production of GUVs (Pott et al. 2008). However, we found that at the highest voltages (350 and 450 mV) a larger fraction of multilamellar and defective vesicles was observed (fig. 5B). Therefore, in our hands the best trade-off between GUV quality and efficient binding of septins was achieved for a growth time of 6 hours and voltage of 350 mV. However, the growth time can be extended up to 16 hours by decreasing the voltage to 250 mV approximately, yielding comparable GUV quality and level of septins binding.

Finally, we tested the influence of the buffer composition, glucose and ionic strength concentrations. In experiments where GUVs are prepared in a buffer containing sucrose, the

external buffer often contains glucose to increase the optical contrast in phase contrast microscopy and to facilitate sedimentation. To prevent any GUV bursting, the osmolarity of both buffers must be matched. We found that above 300 mM glucose in the external buffer, the binding of septins was inhibited. What induces this effect is unclear but it has been shown that similarly, at high concentration, sugars inhibit the interactions between biotin and streptavidin (Houen and Hansen 1997). In contrast, varying the monovalent salt (NaCl) concentration from 150 to 400 mM did not affect binding of septins to vesicles (approximately 4000 septins.μm^{-2}) (data not shown). The interaction was thereby barely screened by electrostatic effects, which argues for the high specificity of the PI(4,5)P2 – septin interaction.

As a conclusion, in our hands, the optimal protocol to produce GUVs doped with PI(4,5)P2 was: 4-5 µL of the lipid mixture containing EPC, 10 % DOPS, 10 % DOPE, 15 % cholesterol and 8 % PI(4,5)P2 spotted on two platinum wires. Droplet were dried for 30 minutes under vacuum. The GUVs growth was performed in 10 mM Tris pH 7.6, 50 mM NaCl and 50 mM sucrose under an AC voltage of 350 mM at 500 Hz during 6 hours.

3.4 PI(4,5)P2-containing GUVs have to be used within a short time frame

Within the time course of our assays, we noticed that the septins-GUVs interaction decreased and no reproducible results were obtained when the time period between the preparation of GUVs and the binding experiments was extended. Indeed, we observed that within a period of two hours, the interaction declined to be suppressed after 3.5 hours (Table 3).

This drop in interaction can result e.g. from the solubilization of PI(4,5)P_2 from the membrane to the buffer solution as already suggested by Carvalho et al (Carvalho et al. 2008), or from a chemical degradation. To test the first hypothesis, we produced GUVs doped with a red fluorescent PI(4,5)P2. Figure 6.A displays the variation of fluorescence with time in the bilayers, thus the PI(4,5)P2 concentration in the GUVs. The fluorescence decreased by about 40%, 3 hours after the GUVs have been transferred in the observation chamber (Fig 6.A, black curve). As a control, another fluorescent lipid (Bodipy-TR-Ceramide) was used and we did not observe a significant variation of the fluorescence intensity of the GUVs over the same time scale (Fig 6.A, red curve). This observation ruled out any bleaching effect. We then produced two distinct batches of GUVs containing either red or green fluorescent PI(4,5)P2 and incubated both populations together. Three hours after their injection in the chamber, the red GUVs contained a high fraction of green PI(4,5)P2 and vice versa (fig. 6.B). Taken together, those

observations demonstrated that the PI(4,5)P2 can partition between the membrane of the GUVs and the bulk solution and thus, can be exchanged between vesicles .

Next, we tested the degradation of PI(4,5)P2 over time (between 0 and 5 hours) in an aqueous buffer by performing state-of-the-art mass spectrometry lipodomics experiments. Pure PI(4,5)P2 solutions were flash frozen at different time points after their solubilization in buffer (Tris 10 mM, pH 8). We measured the relative amount of PI(4,5)P2 as well as the amount of PIP generated by the possible hydrolysis of PI(4,5)P2. The absolute values generated by the analysis are not quantitative per se. Hence, from the data one can only infer and compare the evolution of the amount of a given lipid specie at the different assayed time points. The measurements for PIP and PI(4,5)P_2 are performed independently using a lipid standard (see material and method section) specific for each analyzed lipid. The results are plotted in figure 6.C for both PIP and PI(4,5)P_2. Both the amount of PI(4,5)P2 and PIP remained rather constant at about 250 and 3 (arbitrary units) for PI(4,5)P_2 and PIP respectively. The mild decrease of PI(4,5)P2 and increase of PIP relative abundance remained within experimental errors (20%). Hence, most of the PI(4,5)P2 was intact over time. A small fraction of PIP is already present right after the resolubilization of the dried lipid film into the buffer. However, with time, the relative amount of PIP remained stable.

In this report, we described four main observations: First, the septin–PI(4,5)P2 interaction is highly specific. Second, the comparison of three common methods for producing GUVs demonstrates that electro-formation on non-planar platinum wires is the most appropriate to form GUVs containing PI(4,5)P2. Third, the incorporation and stability of PI(4,5)P2 depend on multiple parameters. Fourth, the budding yeast septin binding onto GUVs significantly drops with time.

4- DISCUSSION

4.1 PI(4,5)P2 incorporation into GUVs is enhanced in the presence of monovalent salt

Using the binding of septins as a readout, we show that two methods, electro-formation on platinum wires and gel-assisted swelling on PVA are suitable for incorporation of PI(4,5)P2 in the GUVs membrane. In contrast, GUVs grown by electro-formation on ITO plates are unable to bind septins. The former two protocols include salt at a significant concentration. This suggests that a monovalent salt concentration of 50 mM is necessary to incorporate PI(4,5)P2 lipids within vesicles.

Indeed, the net charge of PI(4,5)P2 can vary from -3 to -5, depending on pH. The pKa values of the phosphate groups at the positions 4' and 5' of the inositol group are respectively 6.7 and 7.7. In our conditions (pH 7.6), the charge density of PI(4,5)P2 might prevent an efficient incorporation into a bilayer because of electrostatic repulsions between polar lipid head groups. Moreover, the negative charge of PI(4,5)P2 renders this lipid much more soluble in solution than other phospholipids. As reported, the critical micelle concentration (CMC) of PI(4,5)P2, thus its solubility in solution, decreases with the ionic strength: 200 μM in pure water, 30 μM in 50 mM PIPES or Tris (pH 7) (Palmer 1981) and 2 μM in 100 mM NaCl (Walsh et al. 1995), and favors a stronger partition towards the lipid bilayer. Therefore, as shown here, methods of formation of GUVs in the presence of salt, electro-formation on platinum wire and swelling on PVA favored higher PI(4,5)P2 concentration in the membranes and consequently, a stronger septin binding.

Moreover, the presence of monovalent salts even at 50 mM partially screens these repulsions. It has been shown that divalent salts, in particular calcium and magnesium, play an important role in the reorganization of membrane containing PI(4,5)P2 as they induce clusters of PI(4,5)P2 in membranes (Braunger et al. 2013; Wang et al. 2012; Carvalho et al. 2008; Levental et al. 2009). The role of monovalent salts has been less studied. However, in the absence of multivalent cations, the distribution of PI(4,5)P2 has been proposed to depend on the electrostatic balance between attractive and repulsive forces caused by hydrogen bond network between headgroups (Wang et al. 2014). Moreover, the clustering of PI(4,5)P2 lipids has been proposed to be a combination of hydrogen bonding between lipid head groups and electrostatic interaction which appear to prevail (Ellenbroek et al. 2011; Wang et al. 2012). To incorporate PI(4,5)P2 efficiently within lipid supported bilayers, Braunger et al. (Braunger et al. 2013) have proposed a method which uses lower pH (4.8) and citrate buffers to decrease the net charge of the PI(4,5)P2 heads and thereby to lower the electrostatic repulsions. Surprisingly, Carvalho et al.(Carvalho et al. 2008) were able to produce GUVs containing PI(4,5)P2 in the absence of salt with electro-formation on ITO growing conditions similar to ours and lipid composition DOPC with PI(4,5)P2. These discrepancies might result from different PI(4,5)P2 binding reporter proteins, ezrin versus septin. Ezrin might be less sensitive and specific than septins to PI(4,5)P2 interaction for its membrane binding.

In addition, the enhanced incorporation of PI(4,5)P2 by electro-formation using platinum wires versus ITO plates might originate from the higher frequency (500 Hz vs 1Hz) applied on platinum wires than on ITO plates. Hence, the better incorporation of PI(4,5)P2 using platinum

wires would be the result of the screening of electrostatic repulsion combined with a higher frequency applied throughout GUVs growth.

4.2 GUVs containing PI(4,5)P2 have to be used quickly.

Septins bind particularly well to GUVs produced by the gel-assisted method on PVA. However, their production is much less controlled than electro-formation and results in the formation of a significant proportion of defective and multilamellar vesicles, which cannot be used for further quantitative assays. We found that the higher amount of septins bound to vesicles produced by PVA correlates with the high amount of multilamellar vesicles. However, we cannot exclude that septins bind better to these vesicles, because the growth time is shorter and the sensitive PI(4,5)P2 is thereby more preserved. The interaction of septins with GUVs decays with time. Mass spectrometry shows that PI(4,5)P2 does not get significantly degraded over time. Surprisingly, we have shown that PI(4,5)P2 is progressively displaced from the bilayer to the bulk, as evidenced in figures 6 A-B, probably due to its larger aqueous solubility than other less charged phospholipids. In vivo there is a continuous turnover of PI(4,5)P2 and the level of cellular PI(4,5)P2 is regulated by enzymes that hydrolyze, phosphorylate or dephosphorylate this lipid (Xu et al. 2003; Thore et al. 2007). The observed re-solubilization of PI(4,5)P2 reported here is therefore not an issue *in vivo* since PI(4,5)P2 is continuously recycled *in cellulo*.

4.3 Septins bind to PI(4,5)P2 in a preferential manner

Our systematic observations clearly demonstrate a specificity for the septin – PI(4,5)P2 interaction when compared with PLC-δ. In our hands, without PI(4,5)P2, barely any interaction can be detected as previously observed on lipid monolayers (Bertin et al. 2010). Moreover, in high ionic strength conditions (above 300 mM monovalent salt) septins still interact with PI(4,5)P2-containing liposomes. Even though the reinforcement of electrostatic interactions through PS addition facilitates the binding of septins onto vesicles, septins still bind to PI(4,5)P2 when the electrostatic interactions are screened. It has previously been shown that the amino acid basic stretch at the N terminus of Cdc10, the central subunit within the septin complex, is the major domain responsible for this specific protein-lipid interaction (Bertin et al. 2010). We cannot exclude that other domains among which the flexible C terminal coiled coils contribute to the septin-PI(4,5)P2 interaction. However, a recent report suggests that if the C-terminal extension of septins mediates the protein-membrane interaction, this involves an electrostatic

component. In their hands, not significant difference between phosphoinositides or phosphatidylserine PS is detected (Zeraik et al. 2016).

Septins from other organisms do interact with other phosphoinositides (Dolat and Spiliotis 2016). The preferential interaction of budding yeast septins with PI(4,5)P2 might be restricted to S. cerevisiae. We chose to focus on PI(4,5)P2 because we had shown, among several phosphoinositides (PI, PIP2 and PIP3), that PI(4,5)P2 was the only one capable of organizing septins into regular sheets of filaments. Budding yeast septins poorly interacted with PI and interacted but were aggregated on PI(3,4,5)P3 biomimetic membrane (Bertin et al. 2010).

5- CONCLUSION

We have carried out a systematic study to optimize the binding of septins to PI(4,5)P2 containing GUVs. We have established that electro-formation on platinum wires is the most appropriate method to achieve an optimal septin-lipid interaction, and thus the best conditions to maximize the quantity of PI(4,5)P2 in GUVs. We believe that our conclusions are applicable to any PI(4,5)P2-binding protein. Concerning septins, it opens a whole range of possible novel assays that will uncover and dissect the multi-tasking functions of septins. We will now be able to reveal the role of septins in tuning the mechanical properties of membranes and their ability to induce deformations as previously shown by Tanaka-Takiguchi et al. (Tanaka-Takiguchi et al. 2009)

Acknowledgments:

We thank Thibault Lagny for fruitful discussions and Ayako Yamada for her initial contribution to this work, Laura Picas and Bruno Goud for the kind gift of PLC-δ protein. This work benefited from the support of the ANR (project "SEPTIME", ANR-13-JSV8-0002-01). A.Beber and M.A. are funded by the Ecole Doctorale "ED564 : Physique en Ile de France". P. B. group is part of the CNRS consortium CellTiss. P.B and D.L. groups belong to the Labex CelTisPhyBio (ANR-11-LABX0038) and to Paris Sciences et Lettres (ANR-10-IDEX-0001-02).

Figure legends:

Figure 1:

A) Density of septins (black circles) or PLC-δ (red squares) bound on GUVs as a function of PI(4,5)P2 molar fraction incorporated in the GUVs membrane. Intensities are normalized by the value at 10 % PI(4,5)P2. Errors bars are standard deviation.
B) Confocal images of GUVs containing no PIP2 (first two top rows) or 8% PIP2 (last two bottom rows) grown with the platinum wire method. The GUVs were incubated with 100 nM of GFP-septins (First and third rows) in the external buffer or 4.2 μM of GFP PLC-δ (second and last rows). For the top row, when septins are used are reported in the absence of PI(4,5)P2, the contrast was enhanced to display the presence of septins in the solution. The red-lipid signal is visualized with Bodipy-Tr-Ceramide. Left (red) : lipid signal, middle (green) : reporter signal, right : merge. Scale bar: 20μm.

Figure 2:

Fluorescence intensity of septins bound to giant unilamellar vesicles containing 8% PI(4,5)P2 as a function of the bulk septin concentration. The green fluorescent signal of septins recorded by confocal microscopy is used to calculate the septin density (see material and methods). Images were taken less than 3 hours after extraction of the GUVs. Errors bars are standard deviation. The continuous line red line is a sigmoidal fit of the experimental data (Table 1). The corresponding Kd value extracted is Kd = 73 nM ± 9 nM.

Figure 3:

Preparation procedure of GUV prepared with electroformation on ITO slide (A), platinum wire (B) or by swelling on PVA gel (C).

D-E: Confocal images of GUVs prepared with 8% PI(4,5)P2 in the lipid composition, with the three methods: ITO without salt (upper row), Platinum wires (middle rows), gel-assisted method on PVA (bottom row). The experiments were performed in the presence of 50 mM salt (E) or without any salt (D).

The GUVs were incubated with 100 nM of GFP-septins (green signal) in the external buffer. The red-lipid signal is visualized with Bodipy-Tr-Ceramide. Merge of lipids and proteins signal is presented in the 3rd/merge column. For the upper row, the contrast was enhanced for the green signal to highlight the fact that no septins are bound on the ITO grown GUV even though they are present in the solution.

Scale bar: 10 μm. Images were taken less than 3 hours after extraction of the GUVs.

F) Histogram showing the proportion of unilamellar, multilamellar and defective vesicles for gel-assisted on PVA (N = 64) and platinum wires (N = 363) growth.

G) Example of confocal microscopy images of defective (left and middle) and multilamellar (right) vesicles grown with PVA methods before the addition of septins.

Figure 4:

Influence of the growth time on the global GUV quality obtained by platinum wires for a fixed voltage (350 mV). (A) Mean septin density bound on the GUVs as a function of the growth time. (B) Mean radius of GUVs as a function of growth time. (C) Proportion of unilamellar, multilamellar and defective vesicles for different growth times. Errors bars are standard deviations.

Figure 5:

Influence of applied voltage on overall GUVs quality for a fixed growth time (6h). (A) Mean septin density bound to GUVs grown at different voltages. Errors bars are standard deviations (B) Proportion of unilamellar, multilamellar and defective vesicles grown at different voltages.

Figure 6:

Exchange and solubilization of fluorescent PI(4,5)P2 out of the GUV membrane and PI(4,5)P2 degradation with time.

A) Variation of the fluorescence intensity of GUV containing red fluorescent PI(4,5)P2 (Black circle) and Bodipy-TR-Ceramide as a function of time. Whereas Bodipy-TR-Ceramide fluorescent intensity is constant over time, the fluorescent PI(4,5)P2 signal decreases overtime.

B) Incorporation /exchange of green/red labeled PI(4,5)P2 into GUVs containing only red or green labeled PI(4,5)P2 initially. At T = 0h, both population of GUVs were mixed. Green circles: Ratio of green over red fluorescence for initially red GUVs, Red squares: Ratio of red over green fluorescence for initially green GUVs.

C) Mass spectrometry analysis for PIP2 (blue) and PIP (green) at different time points after solubilization. The ratios between the areas of the detection peaks for PIP or PIP2 and the internal standard are plotted. The experiments are carried out with a known 20% error.

Table 1: Biochemical parameters of septins interacting with GUV containing 8% PI(4,5)P2. Data of figure 2 were fitted with a Hill equation: $[Septin\ bound] = \frac{S_{sat}}{\left(\left(\frac{K_d}{[Septin\ bulk]}\right)^n + 1\right)}$ were $[Septin\ bound]$ and $[Septin\ bulk]$ are respectively the septiny density bound to the GUV membrane and in the bulk solution, n is the Hill coefficient and Kd the dissociation constant.

Table 2: Effect of the drying conditions on the mean septin density on GUV membrane containing 8%PI(4,5)P2 with 500 nM septins in the external buffer.

Table 3: Mean septin density on GUV membrane. 500 nM septins is added to the external buffer just after the growth or after 1h30 or 3h30

REFERENCES

Aderem A. 1992. The Marcks brothers: A family of protein kinase C substrates. Cell 71(5):713-16.

Aimon S, Manzi J, Schmidt D, Poveda Larrosa JA, Bassereau P and Toombes GES. 2011. Functional Reconstitution of a Voltage-Gated Potassium Channel in Giant Unilamellar Vesicles. PLoS ONE 6(10):e25529.

Angelova MI, Soléau S, Méléard P, Faucon F and Bothorel P. 1992. Preparation of giant vesicles by external AC electric fields. Kinetics and applications. In: Helm C, Lösche M and Möhwald H, editors. Trends in Colloid and Interface Science VI. Darmstadt: Steinkopff doi:10.1007/BFb0116295 p 127-31.

Bertin A and Nogales E. 2016. Chapter 2 - Preparing recombinant yeast septins and their analysis by electron microscopy. In: Amy SG, editor. Methods in Cell Biology: Academic Press Vol. Volume 136; p 21-34.

Bertin A, McMurray MA, Thai L, Garcia Iii G, Votin V, Grob P, Allyn T, Thorner J and Nogales E. 2010. Phosphatidylinositol-4,5-bisphosphate Promotes Budding Yeast Septin Filament Assembly and Organization. Journal of Molecular Biology 404(4):711-31.

Bertin A, McMurray MA, Grob P, Park S-S, Garcia G, Patanwala I, Ng H-l, Alber T, Thorner J and Nogales E. 2008. Saccharomyces cerevisiae septins: Supramolecular organization of heterooligomers and the mechanism of filament assembly. Proceedings of the National Academy of Sciences 105(24):8274-79.

Braunger JA, Kramer C, Morick D and Steinem C. 2013. Solid Supported Membranes Doped with PIP2: Influence of Ionic Strength and pH on Bilayer Formation and Membrane Organization. Langmuir 29(46):14204-13.

Bridges AA and Gladfelter AS. 2014. Fungal pathogens are platforms for discovering novel and conserved septin properties. Current Opinion in Microbiology 20:42-48.

Bridges AA, Jentzsch MS, Oakes PW, Occhipinti P and Gladfelter AS. 2016. Micron-scale plasma membrane curvature is recognized by the septin cytoskeleton. The Journal of Cell Biology 213(1):23-32.

Bucher P, Fischer A, Luisi PL, Oberholzer T and Walde P. 1998. Giant Vesicles as Biochemical Compartments: The Use of Microinjection Techniques. Langmuir 14(10):2712-21.

Carvalho K, Ramos L, Roy C and Picart C. 2008. Giant Unilamellar Vesicles Containing Phosphatidylinositol(4,5)bisphosphate: Characterization and Functionality. Biophysical Journal 95(9):4348-60.

Catimel B, Schieber C, Condron M, Patsiouras H, Connolly L, Catimel J, Nice EC, Burgess AW and Holmes AB. 2008. The PI(3,5)P2 and PI(4,5)P2 Interactomes. Journal of Proteome Research 7(12):5295-313.

Cha T, Guo A and Zhu XY. 2006. Formation of Supported Phospholipid Bilayers on Molecular Surfaces: Role of Surface Charge Density and Electrostatic Interaction. Biophysical Journal 90(4):1270-74.

Clark J, Anderson KE, Juvin V, Smith TS, Karpe F, Wakelam MJO, Stephens LR and Hawkins PT. 2011. Quantification of PtdInsP3 molecular species in cells and tissues by mass spectrometry. Nat Meth 10.1038/nmeth.1564. 8(3):267-72.

Czogalla A, Grzybek M, Jones W and Coskun Ü. 2014. Validity and applicability of membrane model systems for studying interactions of peripheral membrane proteins with lipids. Biochimica et Biophysica Acta (BBA) - Molecular and Cell Biology of Lipids 1841(8):1049-59.

Di Paolo G and De Camilli P. 2006. Phosphoinositides in cell regulation and membrane dynamics. Nature 10.1038/nature05185. 443(7112):651-57.

Dolat L and Spiliotis ET. 2016. Septins promote macropinosome maturation and traffic to the lysosome by facilitating membrane fusion. The Journal of Cell Biology 214(5):517-27.

Ellenbroek Wouter G, Wang Y-H, Christian David A, Discher Dennis E, Janmey Paul A and Liu Andrea J. 2011. Divalent Cation-Dependent Formation of Electrostatic PIP2 Clusters in Lipid Monolayers. Biophysical Journal 101(9):2178-84.

Evans EA, Skalak R and Weinbaum S. 1980. Mechanics and thermodynamics of biomembranes. American Society of Mechanical Engineers.

Garten M, Aimon S, Bassereau P and Toombes GES. 2015. Reconstitution of a Transmembrane Protein, the Voltage-gated Ion Channel, KvAP, into Giant Unilamellar Vesicles for Microscopy and Patch Clamp Studies. JoVE doi:doi:10.3791/52281(95):e52281.

Gokhale NA, Abraham A, Digman MA, Gratton E and Cho W. 2005. Phosphoinositide Specificity of and Mechanism of Lipid Domain Formation by Annexin A2-p11 Heterotetramer. Journal of Biological Chemistry 280(52):42831-40.

Golub T and Caroni P. 2005. PI(4,5)P₂-dependent microdomain assemblies capture microtubules to promote and control leading edge motility. The Journal of Cell Biology 169(1):151-65.

Hall PA and Russell SH. 2004. The pathobiology of the septin gene family. The Journal of Pathology 204(4):489-505.

Harlan JE, Hajduk PJ, Yoon HS and Fesik SW. 1994. Pleckstrin homology domains bind to phosphatidylinositol-4,5-bisphosphate. Nature 10.1038/371168a0. 371(6493):168-70.

Hartwig JH, Thelen M, Resen A, Janmey PA, Nairn AC and Aderem A. 1992. MARCKS is an actin filament crosslinking protein regulated by protein kinase C and calcium-calmodulin. Nature 10.1038/356618a0. 356(6370):618-22.

Heo WD, Inoue T, Park WS, Kim ML, Park BO, Wandless TJ and Meyer T. 2006. PI(3,4,5)P3 and PI(4,5)P2 Lipids Target Proteins with Polybasic Clusters to the Plasma Membrane. Science 314(5804):1458-61.

Houen G and Hansen K. 1997. Interference of sugars with the binding of biotin to streptavidin and avidin. Journal of Immunological Methods 210(2):115-23.

Kahya N. 2010. Protein–protein and protein–lipid interactions in domain-assembly: Lessons from giant unilamellar vesicles. Biochimica et Biophysica Acta (BBA) - Biomembranes 1798(7):1392-98.

Kunze A, Svedhem S and Kasemo B. 2009. Lipid Transfer between Charged Supported Lipid Bilayers and Oppositely Charged Vesicles. Langmuir 25(9):5146-58.

Kwiatkowska K. 2010. One lipid, multiple functions: how various pools of PI(4,5)P2 are created in the plasma membrane. Cellular and Molecular Life Sciences journal article. 67(23):3927-46.

Lagny TJ and Bassereau P. 2015. Bioinspired membrane-based systems for a physical approach of cell organization and dynamics: usefulness and limitations. Interface Focus 5(4).

Lemmon MA, Ferguson KM, O'Brien R, Sigler PB and Schlessinger J. 1995. Specific and high-affinity binding of inositol phosphates to an isolated pleckstrin homology domain. Proceedings of the National Academy of Sciences of the United States of America 92(23):10472-76.

Levental I, Christian DA, Wang Y-H, Madara JJ, Discher DE and Janmey PA. 2009. Calcium-Dependent Lateral Organization in Phosphatidylinositol 4,5-Bisphosphate (PIP2)- and Cholesterol-Containing Monolayers. Biochemistry 48(34):8241-48.

Liu AP and Fletcher DA. 2006. Actin polymerization serves as a membrane domain switch in model lipid bilayers. Biophys J 91(11):4064-70.

Martin TFJ. 2001. PI(4,5)P2 regulation of surface membrane traffic. Current Opinion in Cell Biology 13(4):493-99.

Moens PDJ and Bagatolli LA. 2007. Profilin binding to sub-micellar concentrations of phosphatidylinositol (4,5) bisphosphate and phosphatidylinositol (3,4,5) trisphosphate. Biochimica et Biophysica Acta (BBA) - Biomembranes 1768(3):439-49.

Morton LA, Yang H, Saludes JP, Fiorini Z, Beninson L, Chapman ER, Fleshner M, Xue D and Yin H. 2013. MARCKS-ED Peptide as a Curvature and Lipid Sensor. ACS chemical biology 8(1):218-25.

Mostowy S and Cossart P. 2012. Septins: the fourth component of the cytoskeleton. Nat Rev Mol Cell Biol 10.1038/nrm3284. 13(3):183-94.

Palmer FBSC. 1981. The phosphatidyl-myo-inositol-4,5-bisphosphate phosphatase from Crithidia fasciculata. Canadian Journal of Biochemistry 59(7):469-76.

Picas L, Viaud J, Schauer K, Vanni S, Hnia K, Fraisier V, Roux A, Bassereau P, Gaits-Iacovoni F, Payrastre B et al. 2014. BIN1/M-Amphiphysin2 induces clustering of phosphoinositides to recruit its downstream partner dynamin. Article. 5:5647.

Pott T, Bouvrais H and Méléard P. 2008. Giant unilamellar vesicle formation under physiologically relevant conditions. Chemistry and Physics of Lipids 154(2):115-19.

Prévost C, Zhao H, Manzi J, Lemichez E, Lappalainen P, Callan-Jones A and Bassereau P. 2015. IRSp53 senses negative membrane curvature and phase separates along membrane tubules. Nature Communications Article. 6:8529.

Pu M, Fang X, Redfield AG, Gershenson A and Roberts MF. 2009. Correlation of Vesicle Binding and Phospholipid Dynamics with Phospholipase C Activity: INSIGHTS INTO PHOSPHATIDYLCHOLINE ACTIVATION AND SURFACE DILUTION INHIBITION. Journal of Biological Chemistry 284(24):16099-107.

Reeves JP and Dowben RM. 1969. Formation and properties of thin-walled phospholipid vesicles. J Cell Physiol 73:49-60.

Rodríguez-Escudero I, Roelants Françoise M, Thorner J, Nombela C, Molina M and Cid Víctor J. 2005. Reconstitution of the mammalian PI3K/PTEN/Akt pathway in yeast. Biochemical Journal 390(Pt 2):613-23.

Rodriguez N, Pincet F and Cribier S. 2005. Giant vesicles formed by gentle hydration and electroformation: A comparison by fluorescence microscopy. Colloids and Surfaces B: Biointerfaces 42(2):125-30.

Rusinova R, Hobart EA, Koeppe RE and Andersen OS. 2013. Phosphoinositides alter lipid bilayer properties. The Journal of General Physiology 141(6):673-90.

Saarikangas J and Barral Y. 2011. The emerging functions of septins in metazoans. EMBO reports 10.1038/embor.2011.193. 12(11):1118.

Sorre B, Callan-Jones A, Manzi J, Goud B, Prost J, Bassereau P and Roux A. 2012. Nature of curvature coupling of amphiphysin with membranes depends on its bound density. Proceedings of the National Academy of Sciences 109(1):173-78.

Tanaka-Takiguchi Y, Kinoshita M and Takiguchi K. 2009. Septin-Mediated Uniform Bracing of Phospholipid Membranes. Current Biology 19(2):140-45.

Thomas CL, Steel J, Prestwich GD and Schiavo G. 1999. Generation of phosphatidylinositol-specific antibodies and their characterization. Biochemical Society Transactions 27(4):648-52.

Thore S, Wuttke A and Tengholm A. 2007. Rapid Turnover of Phosphatidylinositol-4,5-Bisphosphate in Insulin-Secreting Cells Mediated by Ca²⁺ and the ATP-to-ADP Ratio. Diabetes 56(3):818-26.

Uekama N, Sugita T, Okada M, Yagisawa H and Tuzi S. 2007. Phosphatidylserine induces functional and structural alterations of the membrane-associated pleckstrin homology domain of phospholipase C-δ1. FEBS Journal 274(1):177-87.

Walde P, Cosentino K, Engel H and Stano P. 2010. Giant Vesicles: Preparations and Applications. ChemBioChem 11(7):848-65.

Walsh JP, Suen R and Glomset JA. 1995. Arachidonoyl-diacylglycerol Kinase SPECIFIC IN VITRO INHIBITION BY POLYPHOSPHOINOSITIDES SUGGESTS A MECHANISM FOR REGULATION OF PHOSPHATIDYLINOSITOL BIOSYNTHESIS. Journal of Biological Chemistry 270(48):28647-53.

Wang Y-H, Slochower DR and Janmey PA. 2014. Counterion-mediated cluster formation by polyphosphoinositides. Chemistry and Physics of Lipids 182:38-51.

Wang Y-H, Collins A, Guo L, Smith-Dupont KB, Gai F, Svitkina T and Janmey PA. 2012. Divalent Cation-Induced Cluster Formation by Polyphosphoinositides in Model Membranes. Journal of the American Chemical Society 134(7):3387-95.

Weinberger A, Tsai F-C, Koenderink Gijsje H, Schmidt Thais F, Itri R, Meier W, Schmatko T, Schröder A and Marques C. 2013. Gel-Assisted Formation of Giant Unilamellar Vesicles. Biophysical Journal 105(1):154-64.

Xu C, Watras J and Loew LM. 2003. Kinetic analysis of receptor-activated phosphoinositide turnover. The Journal of Cell Biology 161(4):779-91.

Zeraik AE, Staykova M, Fontes MG, Nemuraitė I, Quinlan R, Araújo APU and DeMarco R. 2016. Biophysical dissection of schistosome septins: Insights into oligomerization and membrane binding. Biochimie 131:96-105.

Zhang J, Kong C, Xie H, McPherson PS, Grinstein S and Trimble WS. 1999. Phosphatidylinositol polyphosphate binding to the mammalian septin H5 is modulated by GTP. Current Biology 9(24):1458-67.

Figure 1

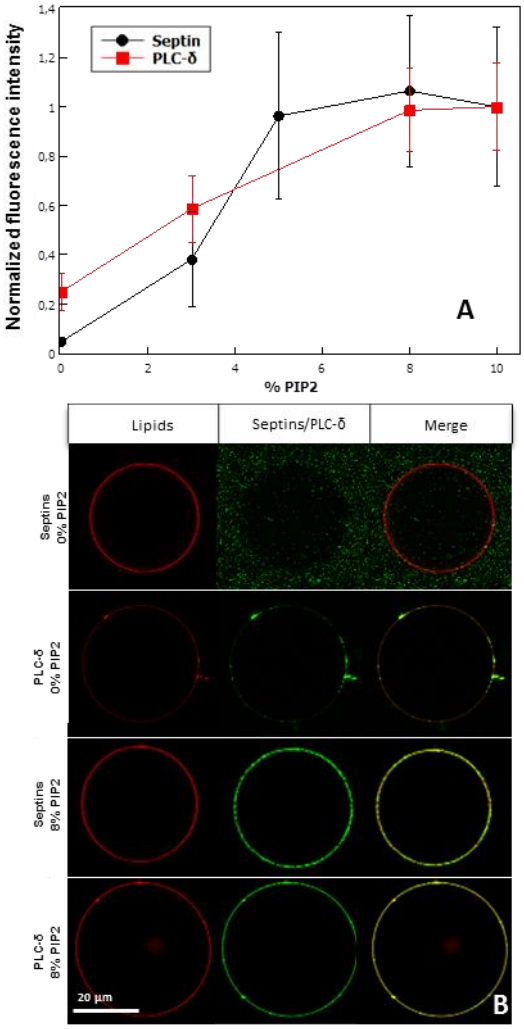
Normalized fluorescence intensity
Septin
PLC-δ
% PIP2
A
Lipids
Septins/PLC-δ
Merge
Septins 0% PIP2
PLC-δ 0% PIP2
Septins 8% PIP2
PLC-δ 8% PIP2
20 µm
B

Figure 2

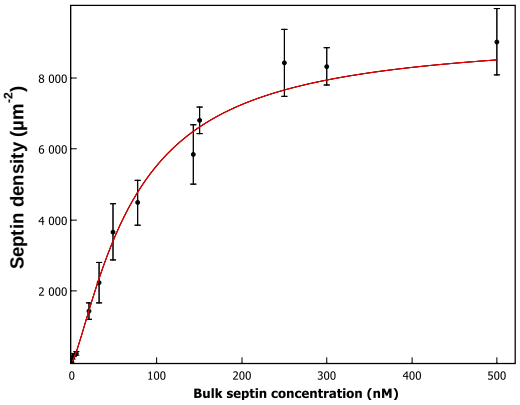
Septin density (µm-2)
8 000
6 000
4 000
2 000
0
100
200
300
400
500
Bulk septin concentration (nM)

Figure 3

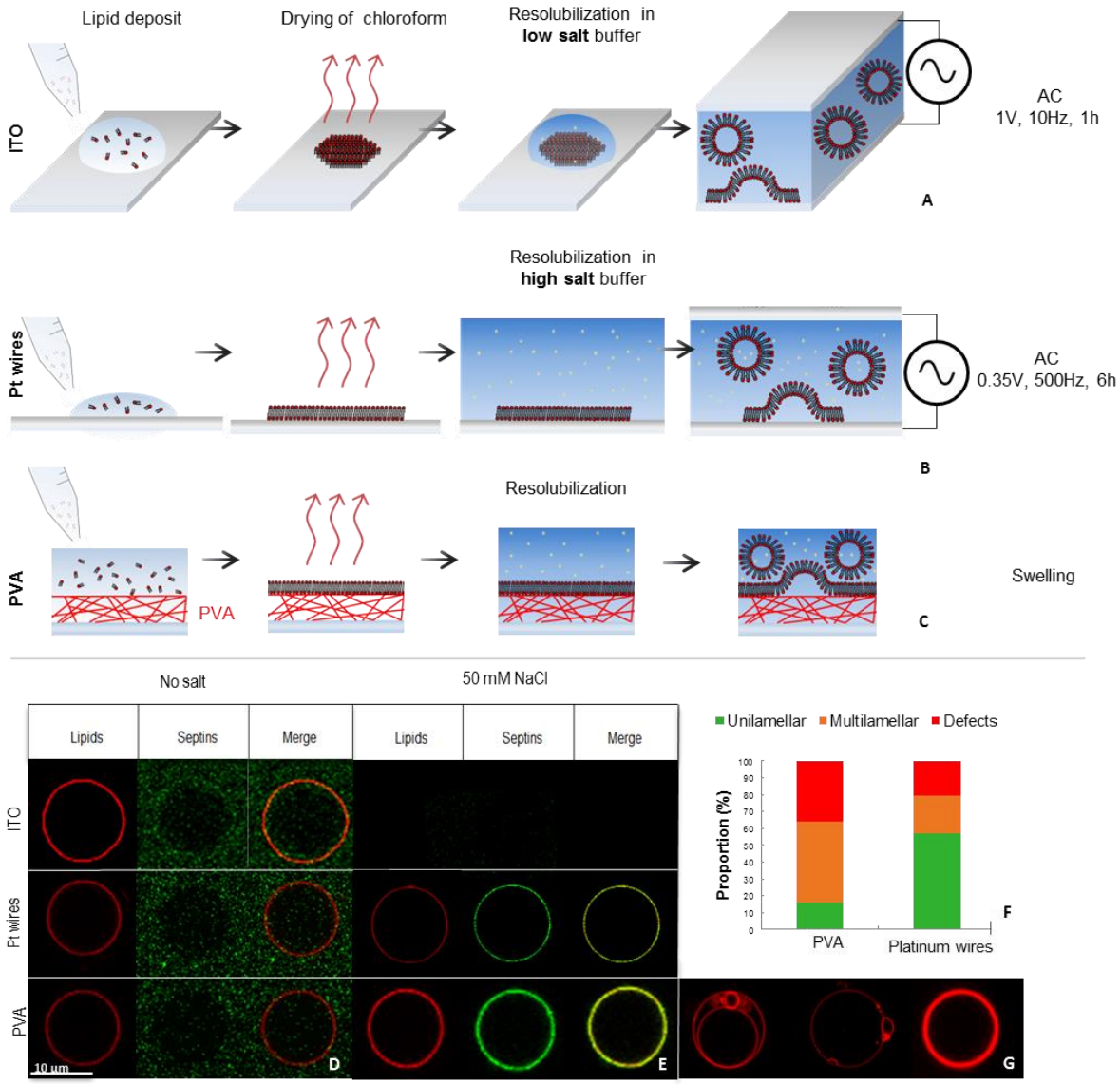
Lipid deposit
Drying of chloroform
Resolubilization in low salt buffer
ITO
AC
1V, 10Hz, 1h
A
Resolubilization in high salt buffer
Pt wires
AC
0.35V, 500Hz, 6h
B
Resolubilization
PVA
PVA
Swelling
C
No salt
50 mM NaCl
Lipids
Septins
Merge
Lipids
Septins
Merge
ITO
Pt wires
PVA
10 µm
D
E
Unilamellar
Multilamellar
Defects
Proportion (%)
PVA
Platinum wires
F
G

Figure 4

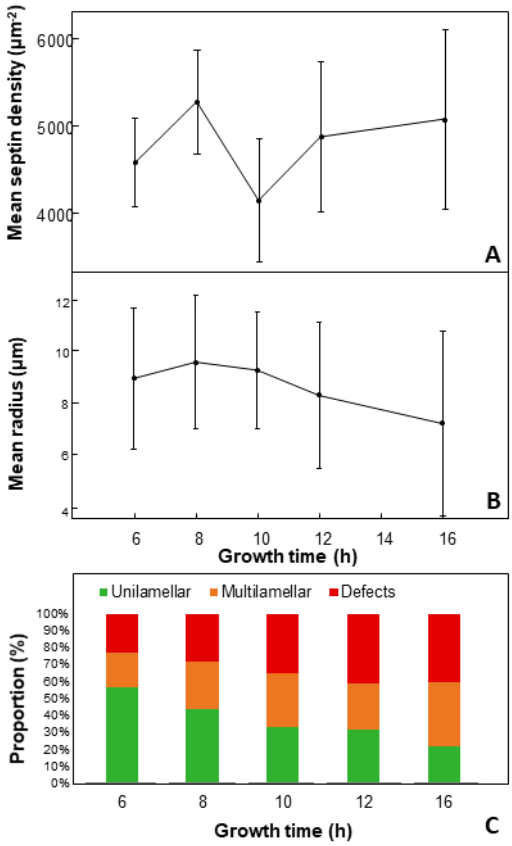
Mean septin density (µm⁻²)
6000
5000
4000
A
Mean radius (µm)
12
10
8
6
4
B
6
8
10
12
14
16
Growth time (h)
Unilamellar
Multilamellar
Defects
Proportion (%)
100%
90%
80%
70%
60%
50%
40%
30%
20%
10%
0%
6
8
10
12
16
Growth time (h)
C

Figure 5

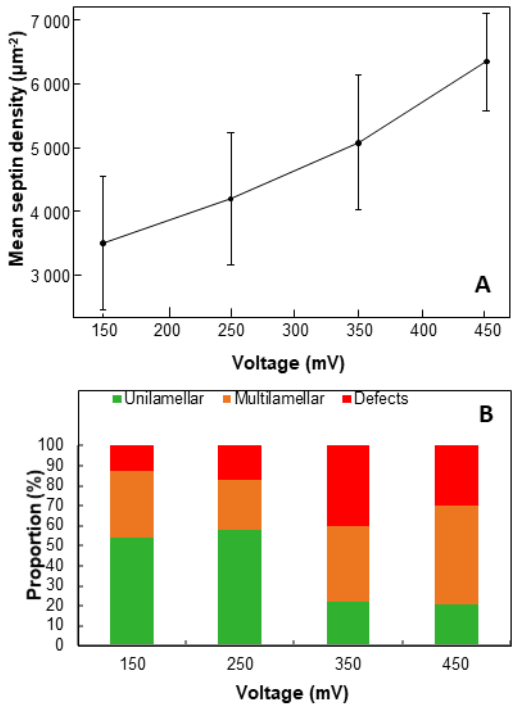
Mean septin density (µm⁻²)
7 000
6 000
5 000
4 000
3 000
A
150
200
250
300
350
400
450
Voltage (mV)
Unilamellar
Multilamellar
Defects
B
Proportion (%)
100
90
80
70
60
50
40
30
20
10
0
150
250
350
450
Voltage (mV)

Figure 6

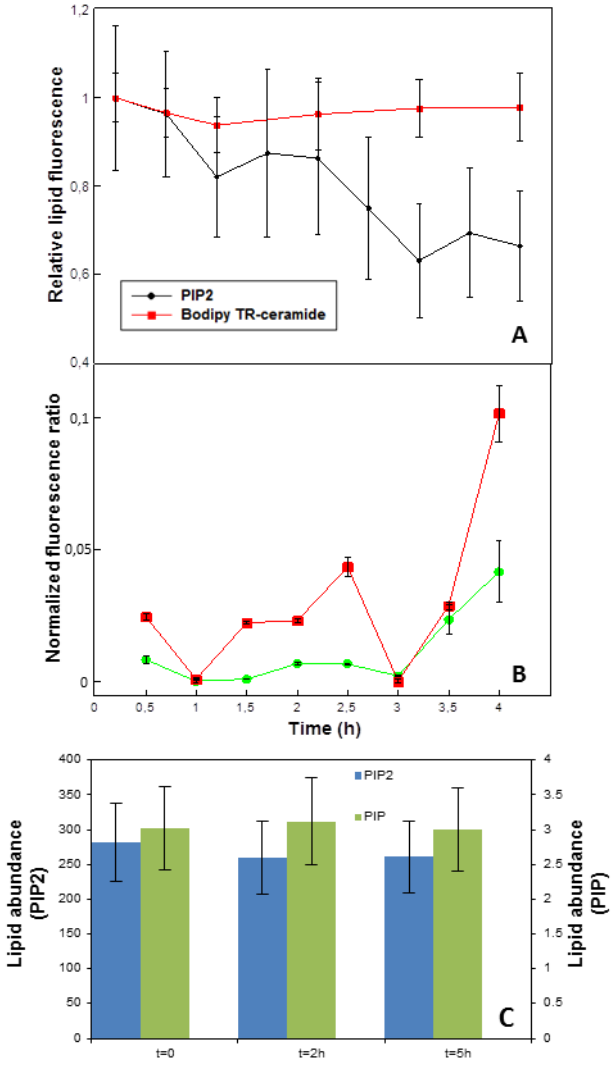
Relative lipid fluorescence
PIP2
Bodipy TR-ceramide
A
Normalized fluorescence ratio
B
Time (h)
Lipid abundance (PIP2)
Lipid abundance (PIP)
PIP2
PIP
C
t=0
t=2h
t=5h

Table 1 :

Saturation concentration	Kd value	Hill coefficient
9200 μm^{-2}	73 nM	1.3

Table 2 :

Drying conditions	Vacuum	Room temperature	60 °C
Mean protein density (μm^{-2})	5200 ± 600	6400 ± 1000	2400 ± 300

Table 3:

Time after GUV production	0h	1h30	3h30
Mean protein density (μm^{-2})	5200 ± 600	4600 ± 700	950 ± 150